



Cite this: *New J. Chem.*, 2019, 43, 16478

A dual-excitation fluorescent probe Eu^{III}-dtpa-bis(HBT) for hydrazine detection in aqueous solutions and living cells

Wenfang Liu,^{ab} Bingqiang Wang,^d Haishuang Jia,^a Jun Wang^{id}*^a and Youtao Song*^c

Based on the esterification of 2-(2-hydroxyphenyl)benzothiazole (HBT) and a rare-earth metal ion complex Eu^{III}-dtpa, a novel dual-excitation fluorescence probe, Eu^{III}-dtpa-bis(HBT), was developed for the detection of hydrazine (N₂H₄). The structure of dtpa-bis(HBT) was characterized via FT-IR and NMR, and its optical properties were studied via UV-vis absorption and fluorescence spectroscopy. Influencing factors including solution acidity, interfering substances and N₂H₄ concentrations were considered for the detection of N₂H₄ using Eu^{III}-dtpa-bis(HBT). Eu^{III}-dtpa-bis(N₂H₄) and HBT emit significant fluorescence at 470 nm ($\lambda_{\text{ex}} = 270$ nm) and 480 nm ($\lambda_{\text{ex}} = 325$ nm), respectively. The detection limit of Eu^{III}-dtpa-bis(HBT) with N₂H₄ was 0.283 μM (14 ppb) and 0.182 μM (9 ppb) upon excitation at 270 nm and 325 nm, which is close to and lower than the EPA standard (10 ppb), respectively. The mechanism for the detection of N₂H₄ by Eu^{III}-dtpa-bis(HBT) was deduced from the experimental results and theoretical calculations. Also, cytotoxicity and cell imaging experiments of Eu^{III}-dtpa-bis(HBT) were performed. The experimental results showed that the fluorescent probe Eu^{III}-dtpa-bis(HBT) can be applied to detect N₂H₄ in aqueous solution and living cells.

Received 31st July 2019,
Accepted 26th September 2019

DOI: 10.1039/c9nj03972d

rsc.li/njc

Introduction

Hydrazine (N₂H₄) is a colorless oily liquid and has a pungent odor, which is similar to that of ammonia. It is widely used in catalysts, pharmaceutical intermediates, emulsifiers, dyes and agriculture.¹ In addition, N₂H₄ is often used as a high-energy propellant for missiles, rockets and satellites due to its high energy density.² However, N₂H₄ is also a potentially carcinogenic toxin. The kidneys, liver, lungs and central nervous system are severely damaged when N₂H₄ is inhaled via the skin, mouth and nose. Obviously, if N₂H₄ is mishandled during its manufacture, use, and transportation, it will not only threaten human health, but also cause serious pollution to the environment. Therefore, it is of great significance to establish convenient and effective methods for the detection of N₂H₄ to control environmental pollution and ensure human health.

In general, the traditional methods for detecting N₂H₄ include titration,³ chemiluminescence,^{4,5} liquid chromatography,⁶

spectrophotometry^{7,8} and electrochemical analysis.^{9–16} Although these methods can be used effectively and accurately to detect N₂H₄, they often need special equipment, complex sample processing and handling and are time-consuming. Therefore, the development of convenient, rapid and economical N₂H₄ detection methods is still required. Recently, detection methods based on fluorescence technology have aroused extensive attention owing to its high selectivity, operation simplicity and real-time analysis. N₂H₄ is usually detected using some fluorescent probes containing dicyano,^{17,18} phthalaldehyde,^{19,20} aldehyde²¹ and aliphatic groups.^{22–26} N₂H₄ can also be detected through the Gabriel reaction^{27–31} and hydrazinolysis.^{32–35} However, when these probes are used to detect N₂H₄, only a single excitation wavelength can be used to give the responses, which is easily disturbed by some external factors. Therefore, more precise fluorescence probes need to be developed to overcome the disadvantages of a single excitation wavelength.

As is known, aminopolycarboxylic acids as chelating agents can coordinate with rare-earth metal ions, forming fluorescent probes.^{36–38} In general, most of the rare-earth metal ions can form nine-coordination compounds with aminopolycarboxylic acid ligands.^{39,40} However, dtpa, as an octadentate ligand, can only provide eight coordination atoms to combine with rare earth metal ions. A water molecule as a ninth ligand together with dtpa can coordinate with rare earth metal ions, forming nine-coordinate complexes. Rare earth metal ions are widely

^a College of Chemistry, Liaoning University, Shenyang, Liaoning Province, 110036, China. E-mail: wangjun888tg@126.com, wangjun891@sina.com

^b Department of Chemistry, Baotou Teachers' College, Baotou, Inner Mongolia, 014030, China

^c College of Environment, Liaoning University, Shenyang, Liaoning Province, 110036, China. E-mail: ysong_tg@126.com

^d School of Chemistry and Material Science, Shanxi Normal University, Linfen, Shanxi Province, 041000, China

used in many fields owing to their unique optical properties, such as large Stokes displacement, long fluorescence life and stable optical properties.^{41,42} In addition, in a previous study, a new rare earth metal ion complex-derived dual-excitation fluorescence probe, Tb³⁺-dtpa-bis(fluorescein), was obtained. The formation and fracture of the ester bonds of Tb³⁺-dtpa with fluorescein led to the fluorescence response changes of Tb³⁺-dtpa-bis(fluorescein), realizing the dual-excitation detection of N₂H₄.⁴³ Based on this, it can be expected that 2-(2-hydroxybenzene)benzothiazole (HBT) can also be utilized for designing novel dual-excitation fluorescence probes based on the hydrazinolysis mechanism. Because HBT is easily excited by light, its photoisomerization from the enol form to the keto form occurs by ES IPT, and thus its fluorescence wavelength obviously increases, which results in a large Stokes shift. Therefore, 2-(2-hydroxybenzene)benzothiazole (HBT) is often applied as the fluorescence group in fluorescence probes owing to its stable optical performance, large Stokes shift, high absorption coefficient and high fluorescence quantum yield.^{44–46} In this work, based on the combination of HBT and the Eu^{III}-dtpa complex, a novel dual-excitation fluorescence probe with two signals, Eu^{III}-dtpa-bis(HBT), was designed and developed (Scheme 1).

Firstly, dtpa-bis(HBT) was synthesized through the esterification of dtpa and HBT, and then Eu(NO₃)₃ solution was added to the dtpa-bis(HBT), forming Eu^{III}-dtpa-bis(HBT), and the formed ester bonds can act as recognition sites for N₂H₄. After adding N₂H₄ to Eu^{III}-dtpa-bis(HBT), the ester bonds were destroyed, forming Eu^{III}-dtpa-bis(N₂H₄) and HBT, which are both fluorescent compounds. Eu^{III}-dtpa-bis(N₂H₄) and HBT displayed significant fluorescence at 470 nm ($\lambda_{\text{ex}} = 270 \text{ nm}$) and 480 nm ($\lambda_{\text{ex}} = 325 \text{ nm}$), respectively. The fluorescence intensities of Eu^{III}-dtpa-bis(HBT) is closely related to the concentration of N₂H₄. Eu^{III}-dtpa-bis(HBT) was used to detect N₂H₄ with a low LOD (0.283 μM and 0.182 μM). The frontier molecular orbital energies of dtpa-bis(HBT) and HBT were

calculated *via* the DFT method. The experimental results indicate that the fluorescent probe Eu^{III}-dtpa-bis(HBT) can be applied to detect N₂H₄ in aqueous solutions and living cells.

Experimental

Reagents and instruments

All reagents were obtained from commercial sources (analytical purity, Shanghai Aladdin Biochemical Technology, China). The water used in the experiments was ultra-pure (18.3 M Ω cm). The actual water samples came from reservoirs, tap water and drinking water. Fourier transform infrared (FT-IR) spectra were obtained on an IRAffinity-1, Japan. ¹H NMR and ¹³C NMR spectra were measured on a Bruker AVANCE NEO with DMSO-*d*₆ as the solvent and TMS as the internal standard. UV-vis absorption spectra were measured on a Cary 50, Varian, USA. Fluorescence spectra were measured on a Cary 300, Varian, USA. All fluorescence imaging experiments were performed on a BIO-RADiMark, ShangHai.

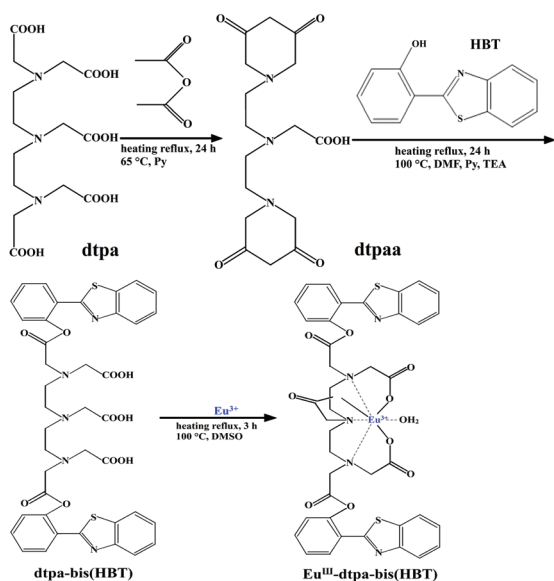
Synthesis of Eu^{III}-dtpa-bis(HBT)

Diethylenetriamine pentaacetic acid dianhydride (dtpaa).

The synthesis of dtpaa was carried out in the absence of water through the improvement of previous methods.^{47–49} The procedure is described in Scheme 1. Briefly, 7.8015 g dtpa (20.00 mmol) was dissolved in a round-bottom flask with acetic anhydride (8.0 mL, 80.00 mol) and pyridine (10.0 mL, 0.12 mol), which was heated and stirred for 24 h at 65 °C. After the solution cooled to room temperature, the residual solvent was removed using a rotary evaporator. The product was obtained by vacuum filtration and washing with acetyl oxide and anhydrous diethyl ether, respectively, and then dried in under vacuum (6.3758 g, 81%). All experiments were performed at room temperature (25.00 \pm 0.02 °C). FT-IR (KBr, cm⁻¹) of dtpaa: 1642.41, 1772.10, 1821.08, 2341.42, 2820.47 and 2979.80. ¹H-NMR (ppm, 400 MHz, DMSO, δ) of dtpa: 2.45 (t, 8H), 3.30 (s, 10H) and 11.01 (s, 3H). ¹H-NMR (ppm, 400 MHz, DMSO, δ) of dtpaa: 2.59 (t, 4H), 2.74 (t, 4H), 3.30 (s, 2H), 3.70 (s, 8H) and 11.01 (s, 1H).

Synthesis of dtpa-bis(HBT)

dtpa-bis(HBT) was synthesized through the improvement of the previous synthesis methods.^{43,50,51} In the absence of water, 1.9678 g dtpaa (5.56 mmol) was dissolved in DMF (20.0 mL) and TEA (2.33 mL), respectively, and stirred constantly until colorless at 50 °C. Next, 2.4981 g HBT dissolved in DMF (20.0 mL) was added to the above solution of dtpaa dropwise. Finally, the mixture was heated for 24 h at 100 °C and then was left to stand overnight. The residual solvent was removed using a rotary evaporator. The product was obtained by vacuum filtration and washing with ice-water and anhydrous diethyl ether, respectively, and then dried under vacuum (3.2574 g, 73%). All experiments are performed at room temperature (25.00 \pm 0.02 °C). FT-IR (KBr, cm⁻¹): 851, 1150, 1253, 1401, 1623, 1794, 3008, 3301. ¹H NMR (ppm, 400 MHz, DMSO, δ): 11.64 (s, 9H), 8.30–8.23 (m, 5H), 8.15 (dd, *J* = 13.8, 7.9 Hz, 2H), 8.06 (d, *J* = 8.1 Hz, 2H), 8.00–7.82 (m, 16H),



Scheme 1 Synthetic route for Eu^{III}-dtpa-bis(HBT) complex.

7.51–7.35 (m, 3H), 7.35–7.17 (m, 2H), 7.08 (t, $J = 12.2$ Hz, 2H). ^{13}C NMR (ppm, 100 MHz, DMSO, δ): 165.75 (s), 134.67 (s), 132.95 (s), 129.00 (s), 126.94 (s), 125.57 (s), 122.52 (d, $J = 12.2$ Hz), 120.23 (s), 118.76 (s), 117.45 (s), 40.50 (d, $J = 20.9$ Hz).

Preparation of Eu^{III} -dtpa-bis(HBT)

0.1010 g dtpa-bis(HBT) (0.125 mmol) and 0.0558 g $\text{Eu}(\text{NO}_3)_3 \cdot 6\text{H}_2\text{O}$ (0.125 mmol) were dissolved in 60 mL buffer solution (pH = 7.50), and stirred for 3.0 h at 100 °C. Then the mixture was cooled to room temperature. The obtained Eu^{III} -dtpa-bis(HBT) solution was transferred to a 250 mL volumetric flask and was diluted with buffer solution. The 0.5 mM Eu^{III} -dtpa-bis(HBT) solution was stored in a cool, dry place. All experiments were performed at room temperature (25.00 ± 0.02 °C).

Preparation of real samples

In this experiment, the actual water samples came from reservoir exit water, reservoir middle water, tap water and drinking water as research objects. Deionized water was used as the control group. Firstly, sixteen 50 mL volumetric flasks were divided into three groups of five. 5.00 mL Eu^{III} -dtpa-bis(HBT) (0.5 mM) reserve solution was added to each of the above volumetric flasks. Then the reserve solution of N_2H_4 in different concentrations was also added to the above three groups of volumetric flasks. These solutions were calibrated with four real water samples and deionized water to 50 mL. All the experiments were performed at room temperature (25.00 ± 0.02 °C).

Cytotoxicity assay

Initially, BV2 cells were inoculated in 24-well plates, and then the cells were grown in an incubator (37 °C, 5% CO_2 and 95% air) containing Eu^{III} -dtpa-bis(HBT) with concentrations ranging from 0–100 μM for 24 h. Then, 15 μL MTT was added to each well and further cultured for 4.0 h.^{52–54} Finally, the BV2 cells in the 24-well plates were treated with DMSO, and then the culture plates were stirred for 10 min. Cell survival was observed with a LEICA DMI8 fluorescence microscope.

Fluorescence microscopy

BV2 cells were cultivated under the above conditions. The cell images were recorded under a confocal laser scanning microscope in the blue channel. One group of cells was treated with 30 μM Eu^{III} -dtpa-bis(HBT) solution for 3.0 h and the other group was treated with 30 μM Eu^{III} -dtpa-bis(HBT) + N_2H_4 solution for 3.0 h. Before the fluorescence imaging, the cells were washed twice with PBS buffer (pH = 7.2). A fluorescence microscope (Leica DMI8) was used to detect the results.

Results and discussion

FT-IR, ^1H and ^{13}C -NMR of dtpa-bis(HBT)

The FT-IR spectra of dtpa, HBT, dtpa-bis(HBT) and dtpa-bis(N_2H_4) were examined. As shown in Fig. 1(c), the stretching vibration peak of C=O in dtpa-bis(HBT) was located at 1749 cm^{-1} , which displays a slight blue-shift compared with that of dtpa

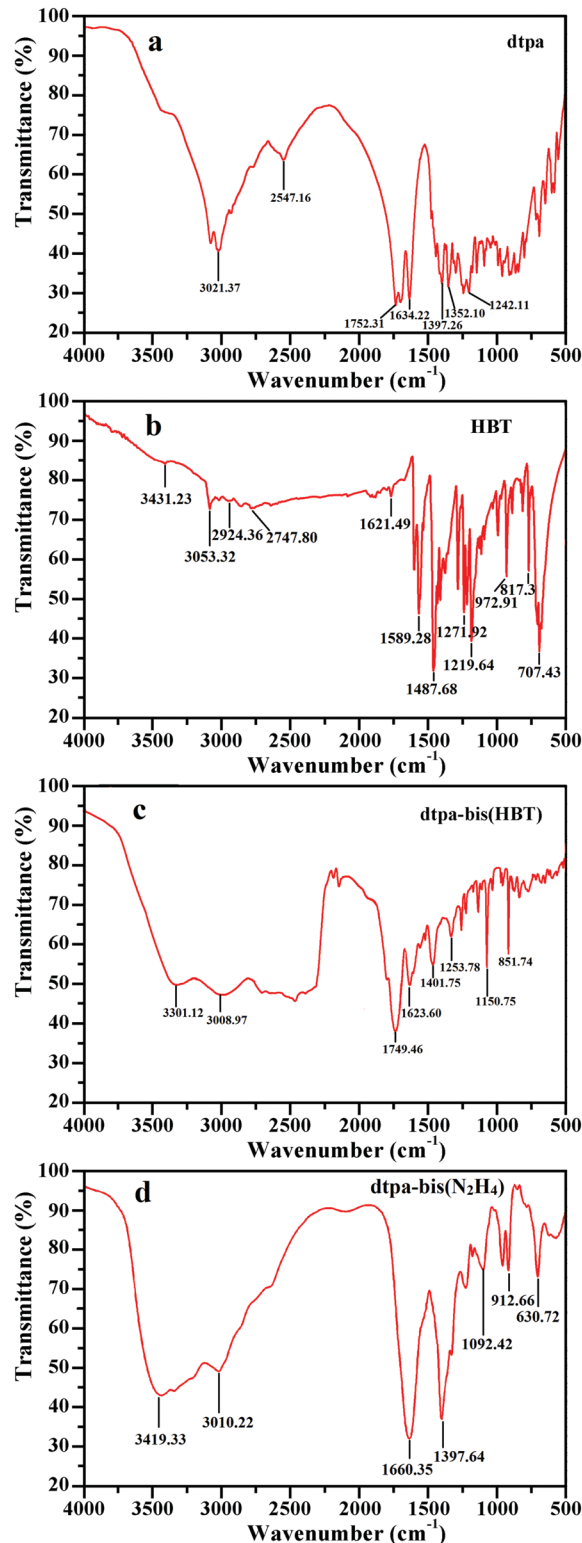


Fig. 1 Infrared spectra of dtpa (a), HBT (b), dtpa-bis(HBT) (c) and dtpa-bis(N_2H_4) (d).

(1752 cm^{-1}) (Fig. 1(a)). This is because the formation of the ester bond provides an electron donor group for the C=O bond, causing the C=O vibration peak to shift to a shorter wavenumber. The asymmetric stretching vibration peak of

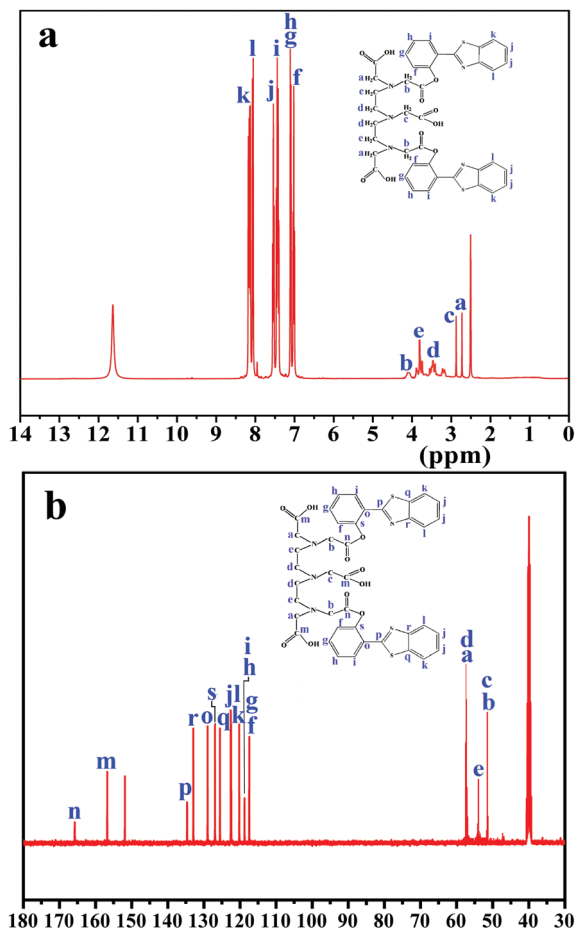


Fig. 2 ^1H NMR (a) and ^{13}C NMR (b) spectra of dtpa-bis(HBT) in $\text{DMSO}-d_6$.

C–O–C in dtpa-bis(HBT) is located at 1254 cm^{-1} , corresponding to dtpa (1352 cm^{-1}) (Fig. 1(a)). Also, the symmetrical stretching vibration peak at 1151 cm^{-1} is ascribed to the C–O–C of dtpa-bis(HBT), corresponding to dtpa (1242 cm^{-1}) (Fig. 1(a)). In addition, the stretching vibration peak at 851 cm^{-1} belongs to the C–H of the aromatic groups in dtpa-bis(HBT). It displays a slight red-shift compared with that of HBT (817 cm^{-1}) (Fig. 1(b)). Because the hydroxyl in HBT is connected with the electron-withdrawing $-\text{COO}-$ group, the electrons are deflected, making the vibration peak of O–H bond move to a longer wavenumber. The shifts of these characteristic peaks prove that dtpa-bis(HBT) was successfully synthesized by esterification between dtpaa and HBT. Furthermore, as shown in Fig. 1(d), the stretching vibration peak at 3419 cm^{-1} is assigned to the N–H in dtpa-bis(N_2H_4). Also, the stretching vibration peak at 1660 cm^{-1} is assigned to the C=O of the amide groups in dtpa-bis(N_2H_4), which presented a blue-shift compared with that of dtpa (1752 cm^{-1}) (Fig. 1(a)). This demonstrates that dtpa-bis(N_2H_4) was generated through the hydrazinolysis between dtpa-bis(HBT) and N_2H_4 .

The components and structure of dtpa-bis(HBT) were confirmed further by ^1H and ^{13}C NMR. In the ^1H -NMR in Fig. 2(a), the $-\text{CH}_2$ protons near the ester groups in dtpa-bis(HBT) appeared at $\delta = 4.05\text{ ppm}$, which displays obvious displacements

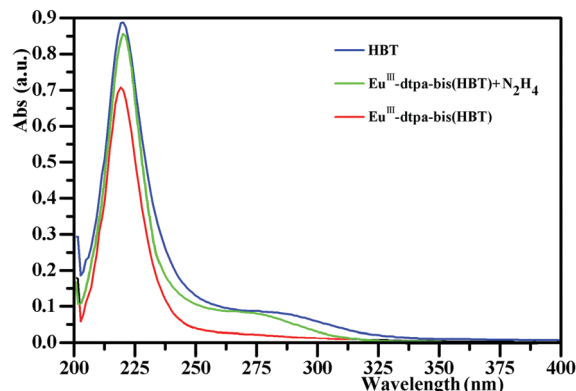


Fig. 3 UV-vis absorption spectra of HBT, Eu^{III} -dtpa-bis(HBT) and Eu^{III} -dtpa-bis(HBT) + N_2H_4 in aqueous solution ($[\text{Eu}^{\text{III}}\text{-dtpa-bis(HBT)}] = 50\text{ }\mu\text{M}$, $[\text{N}_2\text{H}_4] = [\text{HBT}] = 100\text{ }\mu\text{M}$, $[\text{Tris-HCl/DMSO}] = 10\text{ mmol L}^{-1}$, $\text{pH} = 7.50$, $V_{\text{(water)}}/V_{\text{(DMSO)}} = 9:1$ and $T_{\text{solu}} = 25.00 \pm 0.02\text{ }^\circ\text{C}$).

compared with that (3.30 ppm) of the $-\text{CH}_2$ near the carboxyl in dtpa. This is due to the formation of ester bonds between dtpaa and HBT, causing changes in the chemical displacements. Generally, the signal peaks at 172.43 ppm belong to the carbon atoms of $-\text{COOH}$ in dtpa.³⁸ As shown in Fig. 2(b), for the synthesized dtpa-bis(HBT), an obvious signal peak appears at 165.75 ppm , which is assigned to the carbon atoms of the $-\text{C}=\text{O}$ in the ester groups. The appearance of these two characteristic signals (at $\delta = 4.05\text{ ppm}$ in ^1H -NMR and at $\delta = 165.75\text{ ppm}$ in ^{13}C -NMR) demonstrates that dtpa-bis(HBT) was successfully synthesized.

Spectroscopic properties of Eu^{III} -dtpa-bis(HBT)

The UV-vis absorption spectra of HBT, Eu^{III} -dtpa-bis(HBT) and Eu^{III} -dtpa-bis(HBT) + N_2H_4 solutions are presented in Fig. 3. The Eu^{III} -dtpa-bis(HBT) solution at 220 nm has a weak absorption band. However, after the addition of N_2H_4 , the absorption band of the Eu^{III} -dtpa-bis(HBT) solution was obviously enhanced. The results show that hydrazinolysis occurred between Eu^{III} -dtpa-bis(HBT) and N_2H_4 , following the formation of HBT and the Eu^{III} -dtpa-bis(N_2H_4) complex.

The fluorescence spectra of the HBT, Eu^{III} -dtpa-bis(HBT) and Eu^{III} -dtpa-bis(HBT) + N_2H_4 solutions were determined upon excitation at 270 nm and 325 nm . As can be seen in Fig. 4(a), the HBT solution at 470 nm ($\lambda_{\text{ex}} = 270\text{ nm}$) has a strong fluorescence emission peak, but Eu^{III} -dtpa-bis(HBT) only shows a weak fluorescence emission peak. This is because Eu^{III} -dtpa and HBT are coupled by an ester bond to form Eu^{III} -dtpa-bis(HBT) with weak fluorescence. However, after N_2H_4 was added to the Eu^{III} -dtpa-bis(HBT) solution, the Eu^{III} -dtpa-bis(HBT) + N_2H_4 solution at 470 nm ($\lambda_{\text{ex}} = 270\text{ nm}$) displayed a strong fluorescence emission peak, which is due to the fractured ester bonds in Eu^{III} -dtpa-bis(HBT), releasing the HBT with strong fluorescence. Therefore, Eu^{III} -dtpa-bis(HBT) can be applied to detect N_2H_4 upon excitation at 270 nm .

Analogously, as shown in Fig. 4(b), the Eu^{III} -dtpa-bis(HBT) solution at 480 nm ($\lambda_{\text{ex}} = 325\text{ nm}$) also has a weak fluorescence emission peak, and the HBT solution at 480 nm ($\lambda_{\text{ex}} = 325\text{ nm}$) has a strong fluorescence emission peak. However, the Eu^{III} -dtpa-bis(HBT) + N_2H_4 solution at 480 nm ($\lambda_{\text{ex}} = 325\text{ nm}$) showed

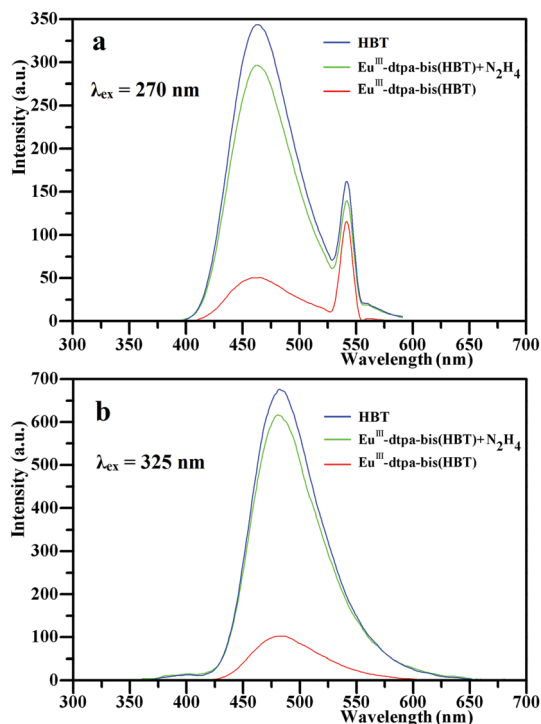


Fig. 4 Fluorescence spectra ($\lambda_{\text{ex}} = 270 \text{ nm}$) (a) and ($\lambda_{\text{ex}} = 325 \text{ nm}$) (b) of Eu^{III} -dtpa-bis(HBT) in the absence and presence of hydrazine (N_2H_4) in aqueous solution ($[\text{Eu}^{\text{III}}\text{-dtpa-bis(HBT)}] = 50.0 \mu\text{M}$, $[\text{N}_2\text{H}_4] = [\text{HBT}] = 100.0 \mu\text{M}$, $[\text{Tris-HCl/DMSO}] = 10 \text{ mmol L}^{-1}$, $\text{pH} = 7.50$, $v_{\text{(water)}/v_{\text{(DMSO)}}} = 9:1$ and $T_{\text{solu}} = 25.00 \pm 0.02 \text{ }^\circ\text{C}$).

a strong fluorescence emission peak after the addition of N_2H_4 to the Eu^{III} -dtpa-bis(HBT) solution. Thus, N_2H_4 can be detected by Eu^{III} -dtpa-bis(HBT) ($\lambda_{\text{ex}} = 325 \text{ nm}$) due to the cleavage of the ester bonds. In summary, the two fluorescence peaks for the synthesized Eu^{III} -dtpa-bis(HBT) appear at 470 nm ($\lambda_{\text{ex}} = 270 \text{ nm}$) and 480 nm ($\lambda_{\text{ex}} = 325 \text{ nm}$). Thus, based on the above experimental results, Eu^{III} -dtpa-bis(HBT) has the potential to detect N_2H_4 at two different excitation wavelengths ($\lambda_{\text{ex}} = 270 \text{ nm}$ and 325 nm).

To compare the fluorescence changes in the Eu^{III} -dtpa-bis(HBT) solution in the presence and absence of N_2H_4 , images of HBT (1), Eu^{III} -dtpa-bis(HBT) (2) and Eu^{III} -dtpa-bis(HBT) + N_2H_4 (3) were photographed under ultraviolet light and visible light, as shown in Fig. 5. Under ultraviolet light, the HBT

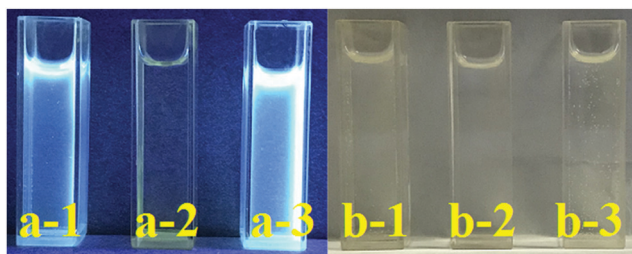


Fig. 5 Fluorescence pictures (ultraviolet-light) (a) and (visible-light) (b) of HBT (1), Eu^{III} -dtpa-bis(HBT) (2) and Eu^{III} -dtpa-bis(HBT) + N_2H_4 (3) ($[\text{HBT}] = [\text{Eu}^{\text{III}}\text{-dtpa-bis(HBT)}] = [\text{Eu}^{\text{III}}\text{-dtpa-bis(HBT)} + \text{N}_2\text{H}_4] = 50.0 \mu\text{M}$, $[\text{Tris-HCl/DMSO}] = 10 \text{ mmol L}^{-1}$, $\text{pH} = 7.50$, $v_{\text{(water)}/v_{\text{(DMSO)}}} = 9:1$ and $T_{\text{solu}} = 25.00 \pm 0.02 \text{ }^\circ\text{C}$).

solution (a-1) showed obvious blue fluorescence, but the Eu^{III} -dtpa-bis(HBT) solution (a-2) did not emit fluorescence. After N_2H_4 was added to the Eu^{III} -dtpa-bis(HBT) solution, the Eu^{III} -dtpa-bis(HBT) + N_2H_4 solution (a-3) displayed obvious blue fluorescence. This is because the ester bonds were cleaved by N_2H_4 , releasing the HBT fluorophore and generating Eu^{III} -dtpa-bis(N_2H_4). However, under visible light, the HBT (b-1), Eu^{III} -dtpa-bis(HBT) (b-2) and Eu^{III} -dtpa-bis(HBT) + N_2H_4 solutions (b-3) were colorless. Therefore, based on the phenomena of the HBT, Eu^{III} -dtpa-bis(HBT) and Eu^{III} -dtpa-bis(HBT) + N_2H_4 solutions under ultraviolet-light, Eu^{III} -dtpa-bis(HBT) can detect N_2H_4 as a dual-excitation fluorescence probe.

The effect of pH on Eu^{III} -dtpa-bis(HBT) for the detection of N_2H_4

The fluorescence responses were studied in Eu^{III} -dtpa-bis(HBT) solution and Eu^{III} -dtpa-bis(HBT) + N_2H_4 mixed solution in the pH range of 2.00 to 11.00. As shown in Fig. 6(a), upon excitation at 270 nm , for the Eu^{III} -dtpa-bis(HBT) solution, the fluorescence response did not change much with an increase in the pH value. In contrast, for the Eu^{III} -dtpa-bis(HBT) + N_2H_4 solution, the fluorescence responses significantly increased with an increase in pH in the range of 2.00 to 6.00. However, when $\text{pH} = 7$, the fluorescence response reached the maximum, and then the fluorescence responses did not change even with a further increase in pH. The experimental results show that under weakly alkaline conditions, hydrazinolysis is occurred

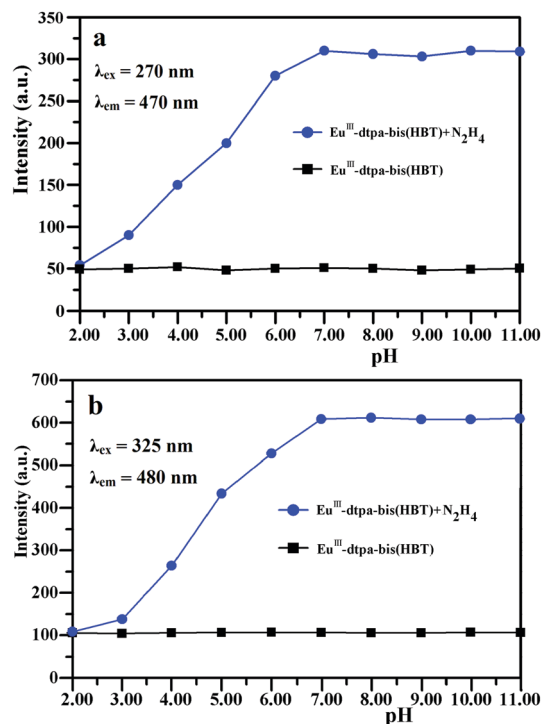


Fig. 6 Fluorescence intensities ($\lambda_{\text{ex}} = 270 \text{ nm}$ and $\lambda_{\text{em}} = 470 \text{ nm}$) (a) and ($\lambda_{\text{ex}} = 325 \text{ nm}$ and $\lambda_{\text{em}} = 480 \text{ nm}$) (b) of Eu^{III} -dtpa-bis(HBT) and Eu^{III} -dtpa-bis(HBT) + N_2H_4 at different pH values (2.00–11.00) ($[\text{Eu}^{\text{III}}\text{-dtpa-bis(HBT)}] = 50.0 \mu\text{M}$, $[\text{N}_2\text{H}_4] = 100.0 \mu\text{M}$, $[\text{Tris-HCl/DMSO}] = 10 \text{ mmol L}^{-1}$, $v_{\text{(water)}/v_{\text{(DMSO)}}} = 9:1$ and $T_{\text{solu}} = 25.00 \pm 0.02 \text{ }^\circ\text{C}$).

between N_2H_4 and Eu^{III} -dtpa-bis(HBT), releasing the HBT fluorophore and producing Eu^{III} -dtpa-bis(N_2H_4).

Similar results were also obtained upon excitation at 325 nm, as shown in Fig. 6(b). The fluorescence responses of the Eu^{III} -dtpa-bis(HBT) solution were almost unchanged in the pH range of 2.00–11.00. For the Eu^{III} -dtpa-bis(HBT) + N_2H_4 solution, the fluorescence responses were enhanced with an increase in pH in the range of 2.00 to 6.00. However, when pH = 7, the fluorescence response reached the maximum, and then the fluorescence responses hardly changed even when the pH was further increased. Apparently, the optimum pH for the detection of N_2H_4 using Eu^{III} -dtpa-bis(HBT) is weak alkalinity upon excitation at both 270 nm and 325 nm.

The selectivity of Eu^{III} -dtpa-bis(HBT) for N_2H_4

It is known that it is of great significance to study the selectivity of a fluorescent probe for the target. Thus, to demonstrate the selectivity of Eu^{III} -dtpa-bis(HBT) to N_2H_4 , the effects of various interferents on the fluorescence responses of Eu^{III} -dtpa-bis(HBT) were investigated. As shown in Fig. 7(a-1), upon excitation at 270 nm, Eu^{III} -dtpa-bis(HBT) only showed a weak fluorescence emission peak. After adding N_2H_4 , the fluorescence response of Eu^{III} -dtpa-bis(HBT) at 470 nm ($\lambda_{em} = 270$ nm) was significantly enhanced, and little effect on the fluorescence responses of Eu^{III} -dtpa-bis(HBT) was observed upon the addition of other interferents. This is because hydrazinolysis occurred between N_2H_4 and Eu^{III} -dtpa-bis(HBT), releasing HBT and producing Eu^{III} -dtpa-bis(N_2H_4), which are both strong fluorescent compounds. The more intuitive comparisons can be seen in Fig. 7(a-2), where in the presence and absence of interferents, no obvious changes were observed for the detection of hydrazine using Eu^{III} -dtpa-bis(HBT).

Similar results were also obtained upon excitation at 325 nm, as shown in Fig. 7(b). For the Eu^{III} -dtpa-bis(HBT) solution, a weak fluorescence response was displayed at 480 nm ($\lambda_{em} = 325$ nm). However, after the addition of N_2H_4 , the fluorescence response of the Eu^{III} -dtpa-bis(HBT) + N_2H_4 solution at 480 nm ($\lambda_{em} = 325$ nm) was enhanced. This is because the hydrazinolysis of Eu^{III} -dtpa-bis(HBT) occurs in the presence of N_2H_4 and the HBT fluorophore is released, resulting in an increase in the fluorescence response. However, after adding other interferents, all the fluorescence responses of the Eu^{III} -dtpa-bis(HBT) solutions at 480 nm barely changed. The corresponding histogram is shown in Fig. 7(b-2), where the fluorescence responses of the Eu^{III} -dtpa-bis(HBT) solutions in the presences of various interferents were almost equal to that of the Eu^{III} -dtpa-bis(HBT) solution. However, after adding N_2H_4 , the fluorescence response of the Eu^{III} -dtpa-bis(HBT) solution was different from that of the others. Thus, these results show that Eu^{III} -dtpa-bis(HBT) can be used to detect N_2H_4 specifically upon excitation at 279 nm and 325 nm.

The anti-interference ability of Eu^{III} -dtpa-bis(HBT) for N_2H_4

The anti-interference ability of Eu^{III} -dtpa-bis(HBT) for various interferents that widely coexist with N_2H_4 in aqueous solutions was tested. As can be seen from Fig. 8(a-1), for the Eu^{III} -dtpa-bis(HBT)

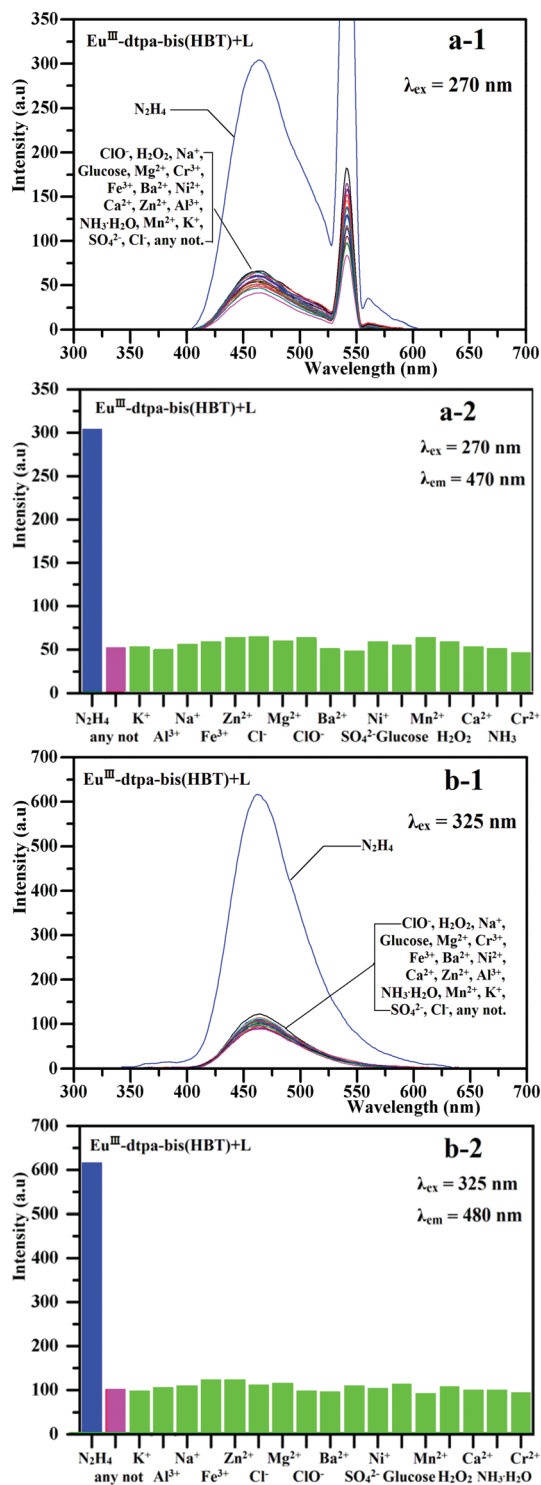


Fig. 7 Fluorescence spectra ($\lambda_{ex} = 270$ nm) (a-1) and ($\lambda_{ex} = 325$ nm) (b-1) and corresponding histograms ($\lambda_{em} = 470$ nm) (a-2) and ($\lambda_{em} = 480$ nm) (b-2) of Eu^{III} -dtpa-bis(HBT) in aqueous solution in the presence of interferents (green bars) and N_2H_4 (blue bar) ($[Eu^{III}\text{-dtpa-bis(HBT)}] = 50.0 \mu\text{M}$, $[\text{interferent}] = 100.0 \mu\text{M}$ and $[N_2H_4] = 100.0 \mu\text{M}$, $[\text{Tris-HCl/DMSO}] = 10 \text{ mmol L}^{-1}$, pH = 7.50, $V_{(\text{water})}/V_{(\text{DMSO})} = 9 : 1$ and $T_{\text{solu}} = 25.00 \pm 0.02 \text{ }^\circ\text{C}$).

solution, a weak fluorescence response was displayed at 470 nm ($\lambda_{em} = 270$ nm). The addition of N_2H_4 caused a dramatic

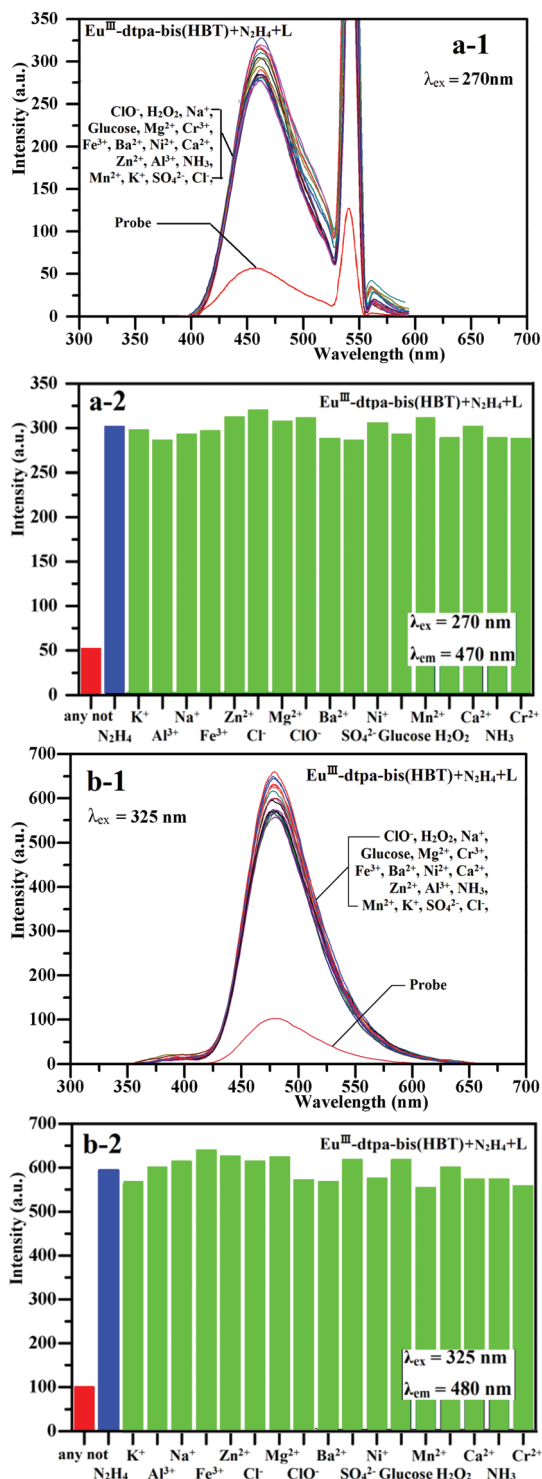


Fig. 8 Fluorescence spectra ($\lambda_{ex} = 270$ nm (a-1) and $\lambda_{ex} = 325$ nm (b-1)) and corresponding histograms ($\lambda_{em} = 470$ nm (a-2) and $\lambda_{em} = 480$ nm (b-2)) of Eu^{III}-dtpa-bis(HBT), Eu^{III}-dtpa-bis(HBT) + N₂H₄ and Eu^{III}-dtpa-bis(HBT) + N₂H₄ + L (L is various interferences (green bars) or N₂H₄ (blue bar)) ([Eu^{III}-dtpa-bis(HBT)] = 50.0 μ M, [interferent] = 100.0 μ M, [N₂H₄] = 100.0 μ M, [Tris-HCl/DMSO] = 10 mmol L⁻¹, pH = 7.50, $v_{(water)}/v_{(DMSO)}$ = 9 : 1 and T_{solu} = 25.00 \pm 0.02 $^{\circ}$ C).

fluorescence response for Eu^{III}-dtpa-bis(HBT), but no prominent fluorescence responses of Eu^{III}-dtpa-bis(HBT) + N₂H₄ were observed after adding other interferences. A more intuitive comparison for the

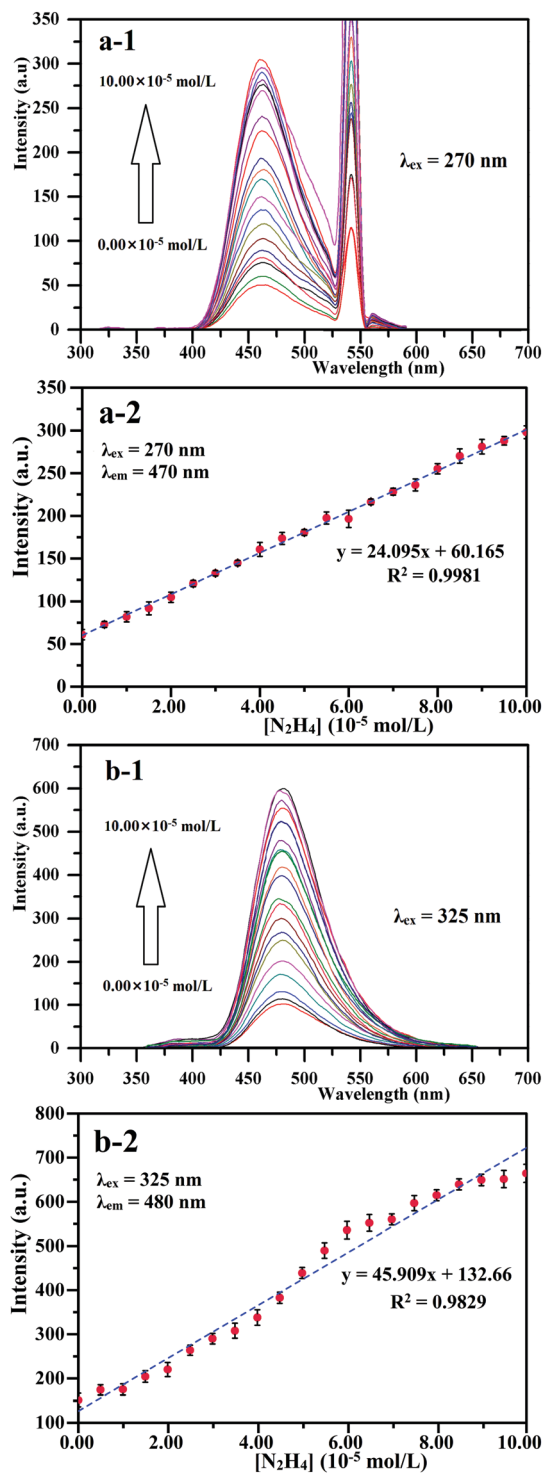


Fig. 9 Fluorescence spectra ($\lambda_{ex} = 270$ nm (a-1) and $\lambda_{ex} = 325$ nm (b-1)) of Eu^{III}-dtpa-bis(HBT) in aqueous solutions with different concentrations of hydrazine (N₂H₄) ranging from 0.00 \times 10⁻⁵ mol L⁻¹ to 10.00 \times 10⁻⁵ mol L⁻¹ and the linear responses of the corresponding fluorescence intensities ($\lambda_{em} = 470$ nm (a-2) and $\lambda_{em} = 480$ nm (b-2)) as a function of hydrazine (N₂H₄) concentration (0.25–75 μ M) ([Eu^{III}-dtpa-bis(HBT)] = 50.0 μ M, [Tris-HCl/DMSO] = 10 mmol L⁻¹, pH = 7.50, $v_{(water)}/v_{(DMSO)}$ = 9 : 1 and T_{solu} = 25.00 \pm 0.02 $^{\circ}$ C).

detection of N₂H₄ using Eu^{III}-dtpa-bis(HBT) in the presence and absence of other interferences can be seen in Fig. 8(a-2). The above

results indicate that Eu^{III} -dtpa-bis(HBT) possesses strong anti-interference ability toward N_2H_4 in the presence of interferents upon excitation at 270 nm.

Similarly, as shown in Fig. 8(b-1), upon excitation at 325 nm, for the Eu^{III} -dtpa-bis(HBT) solution, a weak fluorescence response was displayed at 480 nm ($\lambda_{\text{ex}} = 325 \text{ nm}$). For Eu^{III} -dtpa-bis(HBT) + N_2H_4 solution, the fluorescence response at 480 nm ($\lambda_{\text{ex}} = 325 \text{ nm}$) increased obviously. However, the fluorescence responses of the Eu^{III} -dtpa-bis(HBT) + N_2H_4 solutions containing interferents were almost unchanged. The more intuitive comparisons in Fig. 8(b-2) show that the fluorescence response of Eu^{III} -dtpa-bis(HBT) + N_2H_4 is consistent with that of the Eu^{III} -dtpa-bis(HBT) + N_2H_4 solutions containing different types of interferents. This demonstrates that the Eu^{III} -dtpa-bis(HBT) ($\lambda_{\text{ex}} = 325 \text{ nm}$) also has strong anti-interference ability as fluorescence probe for the detection of N_2H_4 .

Effect of N_2H_4 concentration on the fluorescence responses of Eu^{III} -dtpa-bis(HBT)

The fluorescence responses of Eu^{III} -dtpa-bis(HBT) are closely related to the N_2H_4 concentration. Therefore, it was necessary to study the relationship between the N_2H_4 concentration and the fluorescence responses of Eu^{III} -dtpa-bis(HBT). As shown in Fig. 9(a-1) and (b-1), the fluorescence responses of Eu^{III} -dtpa-bis(HBT) solution at 470 nm ($\lambda_{\text{ex}} = 270 \text{ nm}$) and 480 nm ($\lambda_{\text{ex}} = 325 \text{ nm}$) both increased gradually, respectively, with an increase in N_2H_4 concentration. In addition, as shown in Fig. 9(a-2) and (b-2), excellent linear relationships between the fluorescence responses of Eu^{III} -dtpa-bis(HBT) and N_2H_4 concentration were obtained in the range of 0.25 μM to 75 μM . The corresponding linear equations were $y = 13.207x + 61.172$ ($R^2 = 0.9949$) and $y = 45.909x + 132.66$ ($R^2 = 0.9829$), respectively.

The detection limit of Eu^{III} -dtpa-bis(HBT) for N_2H_4 was about 14 ppb (0.283 μM) ($\lambda_{\text{ex}} = 270 \text{ nm}$) and 9 ppb (0.182 μM) ($\lambda_{\text{ex}} = 325 \text{ nm}$) based on the formula $\text{LOD} = 3\sigma/s$.⁵⁵ Compared with other methods (Table 1), the obtained low detection limit and wide detection range indicate Eu^{III} -dtpa-bis(HBT) can be successfully applied for the quantitative analysis of N_2H_4 .

Mechanism of Eu^{III} -dtpa-bis(HBT) for N_2H_4 detection

Fig. 10 displays two weak fluorescence responses for Eu^{III} -dtpa-bis(HBT) at 470 nm ($\lambda_{\text{ex}} = 270 \text{ nm}$) and 480 nm ($\lambda_{\text{ex}} = 325 \text{ nm}$). After the addition of N_2H_4 , strong fluorescence responses of Eu^{III} -dtpa-bis(HBT) were observed at 470 nm ($\lambda_{\text{ex}} = 270 \text{ nm}$) and 480 nm ($\lambda_{\text{ex}} = 325 \text{ nm}$). The sensing mechanism is due to the occurrence of hydrazinolysis between Eu^{III} -dtpa-bis(HBT) and

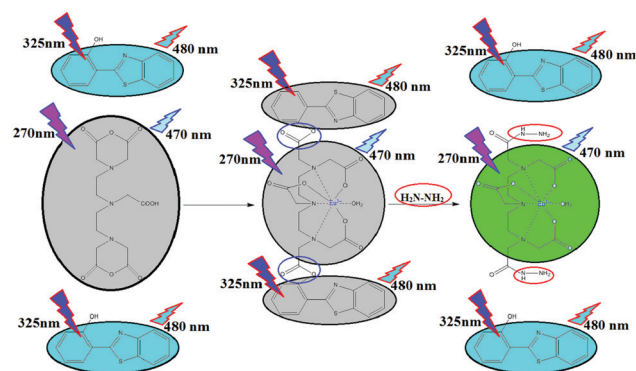


Fig. 10 Reaction mechanism of Eu^{III} -dtpa-bis(HBT) and hydrazine (N_2H_4).

N_2H_4 , releasing the HBT fluorophore and producing Eu^{III} -dtpa-bis(N_2H_4), which are both strong fluorescence compounds. For the detection of N_2H_4 , the Eu^{III} -dtpa-bis(HBT) solution shows excellent anti-interference ability due to the complementary of its two different excitation wavelengths. Therefore, Eu^{III} -dtpa-bis(HBT) as a dual-excitation fluorescence probe can be applied to detect N_2H_4 .

Detection of N_2H_4 in real water samples

To evaluate the feasibility of Eu^{III} -dtpa-bis(HBT) in actual water samples, reservoir exit water, reservoir middle water, tap water and drinking water were selected as research objects, and the concentration of N_2H_4 in the real samples was detected *via* the standard addition method. As shown in Fig. 11(a-1), for Eu^{III} -dtpa-bis(HBT), a weak fluorescence response was displayed at 470 nm ($\lambda_{\text{ex}} = 270 \text{ nm}$).

After different water samples were added to Eu^{III} -dtpa-bis(HBT), almost the same fluorescence responses were obtained for the same concentration of N_2H_4 . However, they all presented a good upward gradient with an increase in the concentration of N_2H_4 in the range of 0.2–1.0 μM . More detailed descriptions are shown in Fig. 11(a-2), where the fluorescence responses of the Eu^{III} -dtpa-bis(HBT) solutions containing the same concentration of N_2H_4 in four water samples were the same and close to that of the control water samples. Therefore, the N_2H_4 in the actual water samples ($\lambda_{\text{ex}} = 270 \text{ nm}$) could be specifically detected using Eu^{III} -dtpa-bis(HBT). As can be seen from Fig. 11(b-1), the fluorescence responses of the Eu^{III} -dtpa-bis(HBT) solutions at 480 nm ($\lambda_{\text{ex}} = 325 \text{ nm}$) increased gradually with an increase in the concentration of N_2H_4 in the four water samples. As shown in

Table 1 Comparison of the proposed method with other reported methods

| Analytical method | LOD (mol L ⁻¹) | Linear range (mol L ⁻¹) | Ref. |
|-------------------------|--|--|-----------|
| Electrodepositing | 0.50×10^{-6} | 2.50×10^{-6} to 5.00×10^{-4} | 14 |
| Chemiluminescence | 2.00×10^{-7} | 5.00×10^{-7} to 1.00×10^{-4} | 4 |
| Spectrophotometry | 1.56×10^{-7} | — | 8 |
| Square wave voltammetry | 0.10×10^{-6} | 0.30×10^{-6} to 7.00×10^{-4} | 15 |
| Electrochemical | 0.08×10^{-6} | 2.00×10^{-6} to 4.00×10^{-5} | 16 |
| Fluorescent probe | 2.83×10^{-7} ($\lambda_{\text{ex}} = 270 \text{ nm}$) | 2.50×10^{-5} to 7.50×10^{-5} | This work |
| | 1.82×10^{-7} ($\lambda_{\text{ex}} = 325 \text{ nm}$) | 2.50×10^{-5} to 7.50×10^{-5} | This work |

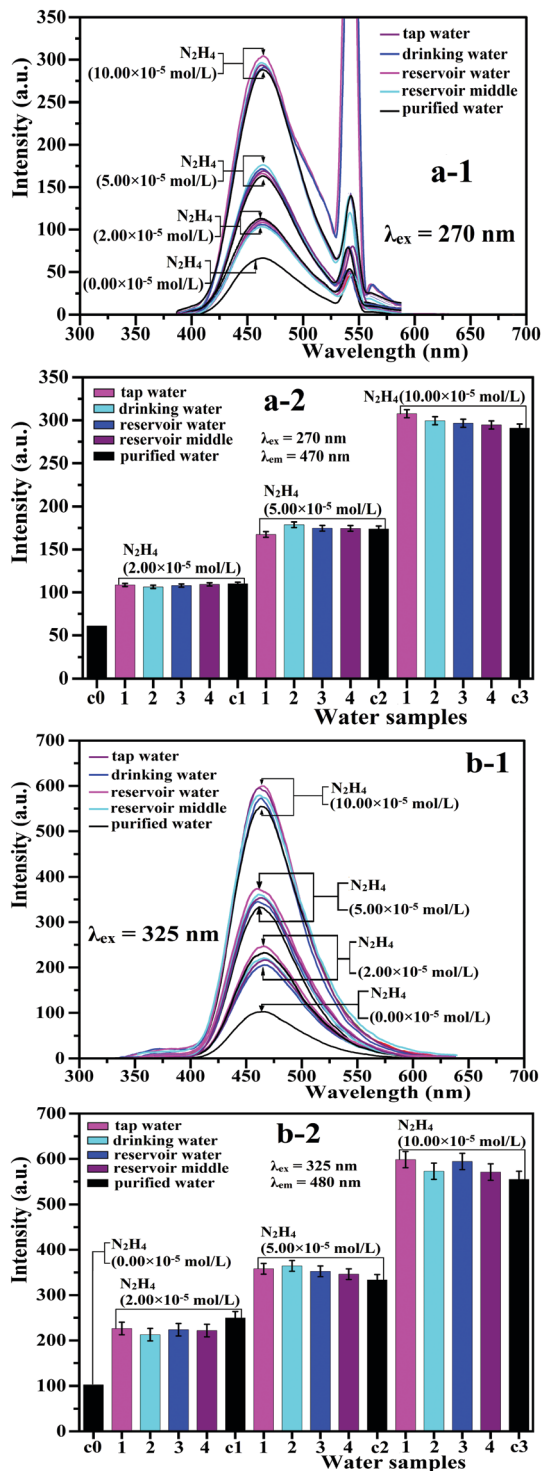


Fig. 11 Fluorescence spectra ($\lambda_{\text{ex}} = 270 \text{ nm}$) (a-1) and ($\lambda_{\text{ex}} = 325 \text{ nm}$) (b-1) and corresponding histograms ($\lambda_{\text{em}} = 470 \text{ nm}$) (a-2) and ($\lambda_{\text{em}} = 480 \text{ nm}$) (b-2) of Eu^{III} -dtpa-bis(HBT) in aqueous solutions with different concentrations of hydrazine (N_2H_4) in four water samples (sample 1: tap water, sample 2: drinking water, sample 3: reservoir exit water and sample 4: reservoir middle water) (c0, c1, c2 and c3: blank groups with corresponding concentrations of hydrazine in purified water [Eu^{III} -dtpa-bis(HBT)] = $50.0 \mu\text{M}$, [Tris-HCl/DMSO] = 10 mmol L^{-1} , pH = 7.50, $v_{(\text{water})}/v_{(\text{DMSO})} = 9:1$ and $T_{\text{solu}} = 25.00 \pm 0.02 \text{ }^\circ\text{C}$).

Table 2 Determined results of the hydrazine (N_2H_4) content in the four water samples with three different concentrations ($\lambda_{\text{ex}} = 270 \text{ nm}$). (Sample 1: tap water, sample 2: drinking water, sample 3: reservoir exit water and sample 4: reservoir middle water)

| Sample | Added (mol L^{-1}) | Found (mol L^{-1}) | Recovery (%) |
|------------|-------------------------------|-------------------------------|--------------|
| Sample-1-1 | 2.00×10^{-5} | 2.01×10^{-5} | 101 |
| Sample-1-2 | 5.00×10^{-5} | 4.45×10^{-5} | 89 |
| Sample-1-3 | 10.00×10^{-5} | 10.27×10^{-5} | 103 |
| Sample-2-1 | 2.00×10^{-5} | 1.92×10^{-5} | 96 |
| Sample-2-2 | 5.00×10^{-5} | 4.92×10^{-5} | 98 |
| Sample-2-3 | 10.00×10^{-5} | 9.93×10^{-5} | 99 |
| Sample-3-1 | 2.00×10^{-5} | 1.98×10^{-5} | 99 |
| Sample-3-2 | 5.00×10^{-5} | 4.75×10^{-5} | 95 |
| Sample-3-3 | 10.00×10^{-5} | 9.81×10^{-5} | 98 |
| Sample-4-1 | 2.00×10^{-5} | 2.04×10^{-5} | 102 |
| Sample-4-2 | 5.00×10^{-5} | 4.74×10^{-5} | 95 |
| Sample-4-3 | 10.00×10^{-5} | 9.73×10^{-5} | 97 |

Fig. 11(b-2), the detection effectiveness of the Eu^{III} -dtpa-bis(HBT) solutions containing the same concentration of N_2H_4 in the four different water samples were consistent with that of the control samples. There were differences in the fluorescence responses of Eu^{III} -dtpa-bis(HBT) with a gradual increase in the concentration of N_2H_4 . Therefore, Eu^{III} -dtpa-bis(HBT) can be used to detect N_2H_4 in various water samples upon excitation at 270 nm and 325 nm.

The results of recovery rates tests using the standard addition method are shown in Tables 2 and 3. Good recovery rates were achieved in the range of 87% to 102% for the four different water samples. Therefore, this proves that Eu^{III} -dtpa-bis(HBT) can quantitatively detect a trace amount of N_2H_4 in actual water samples upon excitation at 270 nm and 325 nm.

Theoretical calculation

To demonstrate the sensing mechanism of Eu^{III} -dtpa-bis(HBT) for N_2H_4 , the frontier molecular orbital energies of dtpa-bis(HBT) and HBT were calculated using the DFT-B3LYP/6-31G method. Because Eu^{III} -dtpa-bis(HBT) contains the rare earth metal Eu^{3+} ion, it has a complicated composition and structure. Since the fluorescence change mainly occurs in the dtpa-bis(HBT) part, only the frontier molecular orbitals of dtpa-

Table 3 Determined results of hydrazine (N_2H_4) content in the four water samples with three different concentrations ($\lambda_{\text{ex}} = 325 \text{ nm}$). (Sample 1: tap water, sample 2: drinking water, sample 3: reservoir exit water and sample 4: reservoir middle water)

| Sample | Added (mol L^{-1}) | Found (mol L^{-1}) | Recovery (%) |
|------------|-------------------------------|-------------------------------|--------------|
| Sample-1-1 | 2.00×10^{-5} | 2.03×10^{-5} | 102 |
| Sample-1-2 | 5.00×10^{-5} | 4.91×10^{-5} | 98 |
| Sample-1-3 | 10.00×10^{-5} | 10.14×10^{-5} | 101 |
| Sample-2-1 | 2.00×10^{-5} | 1.74×10^{-5} | 87 |
| Sample-2-2 | 5.00×10^{-5} | 5.05×10^{-5} | 101 |
| Sample-2-3 | 10.00×10^{-5} | 9.58×10^{-5} | 96 |
| Sample-3-1 | 2.00×10^{-5} | 1.98×10^{-5} | 99 |
| Sample-3-2 | 5.00×10^{-5} | 4.78×10^{-5} | 96 |
| Sample-3-3 | 10.00×10^{-5} | 10.04×10^{-5} | 100 |
| Sample-4-1 | 2.00×10^{-5} | 1.94×10^{-5} | 97 |
| Sample-4-2 | 5.00×10^{-5} | 4.65×10^{-5} | 93 |
| Sample-4-3 | 10.00×10^{-5} | 9.54×10^{-5} | 95 |

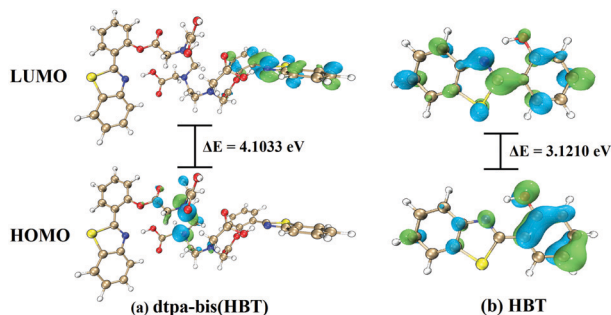


Fig. 12 HOMO–LUMO energy levels and interfacial plots of the molecular orbitals for dtpa-bis(HBT) and HBT.

bis(HBT) were calculated. As can be seen in Fig. 12, the energy differences between the HOMO and LUMO of dtpa-bis(HBT) and HBT were 4.1033 eV and 3.1210 eV, respectively. Because hydrazinolysis occurred between dtpa-bis(HBT) and N_2H_4 , the energy difference (3.1210 eV) between the HOMO and LUMO of produced HBT became lower than that (4.1033 eV) between HOMO and LUMO of dtpa-bis(HBT). It can be seen that the decrease in the energy gap values of HBT compared with that of dtpa-bis(HBT) confirm that HBT is more easily released and emits strong fluorescence.

Cytotoxicity assay

It is great significance to study the cytotoxicity of the fluorescent probe for detecting intracellular N_2H_4 in practical applications. Thus, the effects of different concentrations of Eu^{III} -dtpa-bis(HBT) on its cytotoxicity were investigated *via* the MTT assay on BV2 cells. As shown in Fig. 13, the Eu^{III} -dtpa-bis(HBT) solution exhibited low toxicity to the BV2 cells. Even at a concentration of Eu^{III} -dtpa-bis(HBT) solution of up to 0.5 μM , the survival rate of BV2 cells was 89%. Therefore, demonstrates that Eu^{III} -dtpa-bis(HBT) as a dual-excitation fluorescence probe is a potential substance for cell imaging.

Cellular imaging

The cellular imaging of the detection of N_2H_4 in living cells by Eu^{III} -dtpa-bis(HBT) was evaluated. As shown in Fig. 14(a-1), in the bright field, one group of BV2 cells were treated with

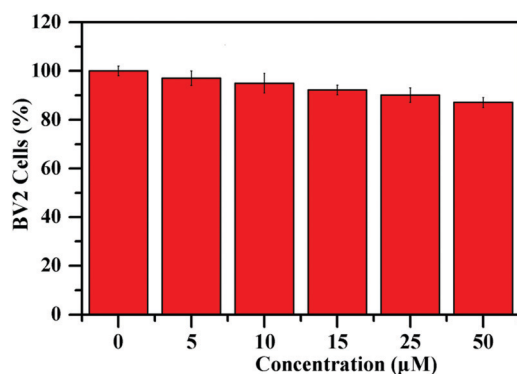


Fig. 13 Calculated viability of BV2 cells in the presence of Eu^{III} -dtpa-bis(HBT) by MTT assay.

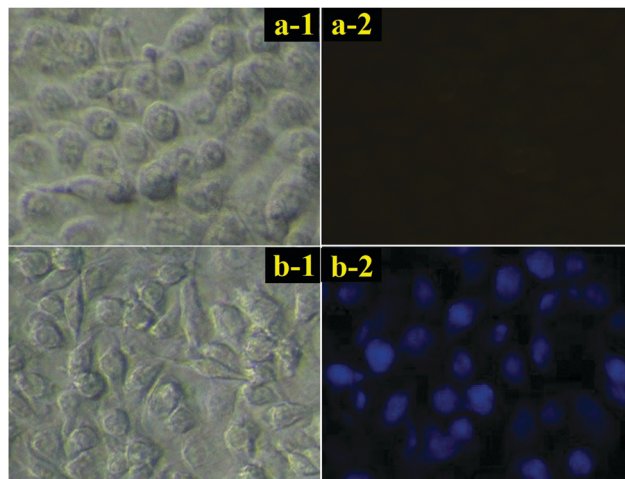


Fig. 14 Bright-field image (1) and fluorescence image (blue light channel) (2) of BV2 cells in the presence of Eu^{III} -dtpa-bis(HBT) (a) and Eu^{III} -dtpa-bis(HBT) + N_2H_4 (b) ($[Eu^{III}\text{-dtpa-bis(HBT)}] = [Eu^{III}\text{-dtpa-bis(HBT)} + N_2H_4] = 30 \mu M$, $[Tris-HCl/DMSO] = 10 \text{ mmol L}^{-1}$, $pH = 7.50$, $V_{(water)}/V_{(DMSO)} = 9 : 1$ and $T_{\text{solv}} = 25.00 \pm 0.02 \text{ } ^\circ C$).

Eu^{III} -dtpa-bis(HBT) (30 μM), which grew normally. However, the size and shape of this group of BV2 cells were different from the other group of BV2 cells that were treated with Eu^{III} -dtpa-bis(HBT) + N_2H_4 (30 μM) (in Fig. 14(b-1)). This suggests that the presence of N_2H_4 affects the normal growth of cells to some extent. As can be seen from Fig. 14(a-2), the BV2 cells were treated with Eu^{III} -dtpa-bis(HBT) (30 μM), which exhibited almost no fluorescence in the blue channel. However, in Fig. 14(b-2), the BV2 cells that were treated with Eu^{III} -dtpa-bis(HBT) + N_2H_4 exhibited obvious blue fluorescence in the blue channel. Thus, these results demonstrate that Eu^{III} -dtpa-bis(HBT) can be applied to detect N_2H_4 in living cells.

Conclusion

In this work, Eu^{III} -dtpa-bis(HBT) as a dual-excitation fluorescence probe, was developed for N_2H_4 sensing. In weakly alkaline conditions, after N_2H_4 was added to Eu^{III} -dtpa-bis(HBT), its ester bonds were cleaved, releasing the HBT fluorophore and producing Eu^{III} -dtpa-bis(N_2H_4), which are both fluorescent compounds. HBT and Eu^{III} -dtpa-bis(N_2H_4) both show relatively strong fluorescence responses at 480 nm ($\lambda_{\text{ex}} = 325 \text{ nm}$) and 470 nm ($\lambda_{\text{ex}} = 270 \text{ nm}$), respectively. Good linear relationships were obtained between the fluorescence responses of Eu^{III} -dtpa-bis(HBT) and N_2H_4 concentrations (0.25–75 μM) with the limit of detection of 14 ppb (0.283 μM) and 9 ppb (0.182 μM), respectively. The theoretical calculation results indicated that HBT is more easily released and emits strong fluorescence. The cytotoxicity and cellular imaging experiments demonstrated that Eu^{III} -dtpa-bis(HBT) can also react with N_2H_4 in living cells.

Conflicts of interest

There are no conflicts to declare.

Acknowledgements

The authors greatly acknowledge the National Science Foundation of China (21371084 and 31570154), Key Laboratory Basic Research Foundation of Liaoning Provincial Education Department (L2015043), Liaoning Provincial Department of Education Innovation Team Projects (LT2015012) and Undergraduate Teaching Reform Projects of Liaoning University (JG2016YB0034) for financial support. The authors also thank our colleagues and other students for their participating in this work.

Notes and references

- H. Lv, H. Sun, S. Wang and F. Kong, *Spectrochim. Acta, Part A*, 2018, **196**, 160–167.
- S. D. Zelnick, D. R. Mattie and P. C. Stepaniak, *Aviation*, 2003, **74**, 1285–1291.
- Z. K. He, B. Fuhrmann and U. Spohn, *Anal. Chim. Acta*, 2000, **409**, 83–91.
- A. Safavi and M. A. Karimi, *Talanta*, 2002, **58**, 785–792.
- A. Safavi, G. Absalan and F. Bamdad, *Anal. Chim. Acta*, 2008, **610**, 243–248.
- A. Salimi, L. Miranzadeh and R. Hallaj, *Talanta*, 2008, **75**, 147–156.
- P. Wuamprakhon, A. Krittayavathananon, N. Ma, N. Phattharasupakun, T. Maihom, J. Limtrakul and M. Sawangphruk, *J. Electroanal. Chem.*, 2018, **808**, 124–132.
- D. Kosyakov, A. Amosov, N. Ul'yanovskii, A. Ladesov, Y. Khabarov and O. Shpigun, *J. Anal. Chem.*, 2017, **72**, 171–177.
- R. B. Channon, M. B. Joseph, E. Bitziou, A. W. T. Bristow, A. D. Ray and J. V. Macpherson, *Anal. Chem.*, 2015, **87**, 10064–10071.
- J. R. Stetter, K. F. Blurton, A. M. Valentine and K. A. Tellefsen, *J. Electrochem. Soc.*, 1978, **125**, 1804–1807.
- J. W. Mo, B. Ogorevc, X. Zhang and B. Pihlar, *Electroanalysis*, 2015, **12**, 48–54.
- Z. Feng, D. Li, L. Wang, Q. Sun, P. Lu, P. Xing and M. An, *Electrochim. Acta*, 2019, **304**, 275–281.
- D. M. Nguyen and Q. B. Bui, *J. Electroanal. Chem.*, 2019, **832**, 444–452.
- G. Wang, C. Zhang, X. He, Z. Li, X. Zhang, W. Lun and B. Fang, *Electrochim. Acta*, 2010, **55**, 7204–7210.
- A. Benvidi, P. Kakoolaki, H. R. Zare and R. Vafazadeh, *Electrochim. Acta*, 2011, **56**, 2045–2050.
- T. Pal, S. Dutta, C. Ray, S. Mallick, S. Sarkar and A. Roy, *RSC Adv.*, 2015, **5**, 51690–51700.
- Y. Liu, D. Ren, J. Zhang, H. Li and X. F. Yang, *Dyes Pigm.*, 2019, **162**, 112–119.
- X. Zheng, S. Wang, H. Wang, R. Zhang, J. Liu and B. Zhao, *Spectrochim. Acta, Part A*, 2015, **138**, 247–251.
- W. Xu, W. Liu, T. Zhou, Y. Yang and W. Li, *J. Photochem. Photobiol., A*, 2018, **356**, 610–616.
- Y. Zhang, Y. Huang, Y. Yue, J. Chao, F. Huo and C. Yin, *Sens. Actuators, B*, 2018, **273**, 944–950.
- J. Wu, J. Pan, Z. Ye, L. Zeng and D. Su, *Sens. Actuators, B*, 2018, **274**, 274–284.
- Y. Qian, J. Lin, L. Han, L. Lin and H. Zhu, *Biosens. Bioelectron.*, 2014, **58**, 282–286.
- M. G. Choi, J. Hwang, J. O. Moon, J. Sung and S. K. Chang, *Org. Lett.*, 2011, **135**, 5260–5263.
- Y. Hao, Y. Zhang, K. Ruan, W. Chen, B. Zhou, X. Tan, Y. Wang, L. Zhao, G. Zhang, P. Qu and M. Xu, *Sens. Actuators, B*, 2017, **244**, 417–424.
- S. Goswami, S. Das, K. Aich, B. Pakhira, S. Panja, S. K. Mukherjee and S. Sarkar, *Org. Lett.*, 2013, **15**, 5412–5415.
- X. Jin, C. Liu, X. Wang, H. Huang, X. Zhang and H. Zhu, *Sens. Actuators, B*, 2015, **216**, 141–149.
- W. D. Wang, Y. Hu, Q. Li and S. L. Hu, *Inorg. Chim. Acta*, 2018, **477**, 206–211.
- L. Cui, C. Ji, Z. Peng, L. Zhong, C. Zhou and L. Yan, *Anal. Chem.*, 2014, **86**, 4611–4617.
- M. V. R. Raju, E. C. Prakash, H. C. Chang and H. C. Lin, *Dyes Pigm.*, 2014, **103**, 9–20.
- X. Dai, Z. Y. Wang, Z. F. Du, J. Y. Miao and B. X. Zhao, *Sens. Actuators, B*, 2016, **232**, 369–374.
- B. Li, Z. He, H. Zhou, H. Zhang, W. Li, T. Cheng and G. Liu, *Dyes Pigm.*, 2017, **146**, 300–304.
- Q. Wu, J. Zheng, W. Zhang, J. Wang, W. Liang and F. J. Stadler, *Talanta*, 2019, **195**, 857–864.
- F. Takashi, S. Satoshi and M. Atsushi, *Biochem. Biophys. Res. Commun.*, 2004, **317**, 77–83.
- Y. Hao, Y. Zhang, K. Ruan, W. Chen, B. Zhou, X. Tan, Y. Wang, L. Zhao, G. Zhang, P. Qu and M. Xu, *Sens. Actuators, B*, 2017, **244**, 417–424.
- Z. Lu, X. Shi, Y. Ma, W. Fan, Y. Lu, Z. Wang and C. Fan, *Sens. Actuators, B*, 2018, **258**, 42–49.
- X. Jiang, F. Tian, F. Yang, X. Dou, J. Wang and Y. Song, *Sens. Actuators, B*, 2017, **238**, 605–612.
- F. Tian, X. Jiang, X. Dou, Q. Wu, J. Wang and Y. Song, *Spectrochim. Acta, Part A*, 2017, **179**, 194–200.
- F. Yang, Z. Yu, X. Li, P. Ren, G. Liu, Y. Song and J. Wang, *Spectrochim. Acta, Part A*, 2018, **203**, 461–471.
- S. Bénazeth, J. Purans, M. C. Chalbot, M. K. Nguyen-Van-Duong, L. Nicolas, F. Keller and A. Gaudemer, *Inorg. Chem.*, 1998, **37**, 3667–3674.
- N. Sakagami, J. I. Homma, T. Konno and K. I. Okamoto, *Acta Crystallogr.*, 1997, **53**, 1378–1381.
- J. Massue, S. J. Quinn and T. Gunnlaugsson, *J. Am. Chem. Soc.*, 2008, **130**, 6900–6901.
- M. Zhang, Z. B. Qu, H. Y. Ma, T. Zhou and G. Shi, *Chem. Commun.*, 2014, **50**, 4677–4679.
- X. Li, Z. Yu, N. Li, H. Jia, H. Wei, J. Wang and Y. Song, *Dyes Pigm.*, 2019, **162**, 281–294.
- M. Zhang, Z. Qu, C. M. Han, L. F. Lu, Y. Y. Li, T. Zhou and G. Shi, *Chem. Commun.*, 2014, **50**, 12855–12858.
- J. E. Kwon and S. Y. Park, *Adv. Mater.*, 2011, **23**, 3615–3642.
- J. Ma, J. Zhao, P. Yang, D. Huang, C. Zhang and Q. Li, *Chem. Commun.*, 2012, **48**, 9720–9722.
- J. M. Couchet, J. Azéma and P. Tisnès, *Inorg. Chem. Commun.*, 2003, **6**, 978–981.

- 48 E. Debroye, S. V. Eliseeva, S. Laurent, L. V. Elst, S. Petoud, R. N. Muller and T. N. Parac-Vogt, *Eur. J. Inorg. Chem.*, 2013, 2629–2639.
- 49 H. H. Shi and Y. S. Yang, *J. Alloys Compd.*, 1994, **207-208**, 29–32.
- 50 A. Bertin, T. Muller, J. L. Gallani and D. Felder-Flesch, *Tetrahedron Lett.*, 2007, **48**, 4699–4702.
- 51 C. Jolley, F. R. Burnet and P. J. Blower, *Appl. Radiat. Isot.*, 1996, **47**, 623–626.
- 52 S. Wang, N. Li, W. Pan and B. Tang, *TrAC, Trends Anal. Chem.*, 2012, **39**, 3–37.
- 53 C. Sun, Y. Wu, P. Wang, G. Zhou, X. Zong, B. Chen and M. Ji, *J. Sol-Gel Sci. Technol.*, 2014, **71**, 211–216.
- 54 Z. Li, W. Zhang, C. Liu, M. Yu, H. Zhang, L. Guo and L. Wei, *Sens. Actuators, B*, 2017, **241**, 665–671.
- 55 G. L. Long and J. D. Winefordner, *Anal. Chem.*, 1983, **55**, 712A–724A.